Distribution Agreement

In presenting this thesis as a partial fulfillment of the requirements for a degree from Emory University, I hereby grant to Emory University and its agents the non-exclusive license to archive, make accessible, and display my thesis in whole or in part in all forms of media, now or hereafter now, including display on the World Wide Web. I understand that I may select some access restrictions as part of the online submission of this thesis. I retain all ownership rights to the copyright of the thesis. I also retain the right to use in future works (such as articles or books) all or part of this thesis.

Anna J. Voss March 22, 2022

Quantitative Identification of Ligand and Receptor Pairs that Drive Astrocyte Development

By

Anna J. Voss

Dr. Steven A. Sloan

Adviser

Neuroscience and Behavioral Biology

Dr. Steven A. Sloan

Adviser

Dr. Michael P. Epstein

Committee Member

Dr. Kristen E. Frenzel

Committee Member

2022

Quantitative Identification of Ligand and Receptor Pairs that Drive Astrocyte Development

By

Anna J. Voss

Dr. Steven A. Sloan

Adviser

An abstract of
a thesis submitted to the Faculty of Emory College of Arts and Sciences of Emory University in partial fulfillment
of the requirements of the degree of
Bachelor of Sciences with Honors

Neuroscience and Behavioral Biology

2022

Abstract

Quantitative Identification of Ligand and Receptor Pairs that Drive Astrocyte Development

By Anna J. Voss

Astrocytes, the most abundant cell-type in the central nervous system (CNS), are star-shaped cells that have numerous roles in CNS physiology including neurotransmitter uptake at the synapse, the formation of the blood brain barrier and regulation of neural circuit formation. Many of these functions are developmentally regulated and are tied to the process of astrocyte maturation, but much remains unknown about the mechanisms that trigger this transformation. An important open question about astrocyte development asks what extrinsic signals cause immature astrocyte progenitors to transition into mature, quiescent cells. We hypothesize that ligands, signaling molecules secreted by other cell types in the brain, regulate astrocyte maturation by binding to receptors on astrocyte progenitors and activating downstream mature astrocyte genes. However, a difficult obstacle is identifying (1) which ligands are present in the developing brain that (2) have cognate receptors expressed in astrocyte progenitors and (3) would likely trigger the expression of mature astrocyte genes. In this study, we use quantitative, genome-wide computational tools to decipher these candidate ligand/receptor pairs whose interactions may initiate astrocyte maturation. Using RNA-Seq data of purified CNS cell populations and NicheNet, an algorithm that computationally matches the regulatory potential of ligands and receptors, we identify ten ligand/receptor pairs with corroborating expression data and whose activation is predicted to mediate expression of mature astrocyte genes. To further refine and confirm the ligands and receptors of interest, we use single-cell human data to add cell type specificity and to more confidently validate the candidacy of putative ligand-receptor pairs. Finally, we use this data to systematically test drivers of astrocyte maturation by exposing

cortical organoids and purified human fetal astrocytes to candidate ligands and use bulk RNA-Seq to observe the ligands' effects on maturation. Understanding how astrocyte maturation occurs may help elucidate their contribution to neurodevelopmental disorders, and the tools we develop in this work can be applied more broadly to understand how cell-cell communication drives cellular processes throughout the human body.

Quantitative Identification of Ligand and Receptor Pairs that Drive Astrocyte Development

By

Anna J. Voss

Dr. Steven A. Sloan

Adviser

A thesis submitted to the Faculty of Emory College of Arts and Sciences of Emory University in partial fulfillment
of the requirements of the degree of
Bachelor of Sciences with Honors

Neuroscience and Behavioral Biology

2022

Acknowledgements

I would like to thank Dr. Michael Epstein for taking a chance on me in high school and providing me with a phenomenal introduction to a research career. Thank you for your invaluable support throughout the past 6 years.

I would like to thank Dr. Steven Sloan for also taking a chance on me my first year at Emory, and for his continued support through the highs, lows, blood (sadly this is literal), sweat, and tears of my project.

I would not be the scientist that I am today without Dr. Epstein's and Dr. Sloan's mentorship, and I will forever be grateful for your belief in me.

I would like to thank Dr. Kristen Frenzel for her mentorship for the past 3 years, and for her advice and support as I completed my undergraduate coursework.

I would like to thank everyone in the Sloan Lab for making this the best lab anyone could ask for. Everyone in this lab has had a positive impact on my life, and I am grateful to have been able to work in such a supportive, fun lab for the past 4 years. I would specifically like to thank Samantha Lanjewar and Caitlin Sojka for their support from the beginning both as lab mates and friends.

Lastly, I would like to thank my family and friends for their support, specifically I would like to thank my parents, sister, grandmother, and Jasmine Lin for listening to me talk about science for extended periods of time.

Table of Contents

Introduction

The development of the mammalian nervous system involves complex choreography and interactions across many diverse cell types. Neuron-glial interactions, particularly, offer an intriguing perspective to studying neurodevelopmental disorders such as autism and schizophrenia (Kim et al., Sawa et al.). However, the signaling between these cell types remains poorly understood. In recent years, however, enormous strides have been taken towards improved understanding of how glia contribute to the formation and function of the developing brain (Reemst et al.).

Astrocytes are the most abundant glial cells in the nervous system, and although we are learning more about their active contribution to central nervous system (CNS) formation and function, much remains unknown about astrocyte development (Molofsky and Deneen). Understanding the origin of these cells is particularly important because of their numerous roles in CNS physiology including neurotransmitter uptake at the synapse (Rose et al), the formation of the blood brain barrier (Kubotera et al.), contributions to synaptogenesis (Baldwin et al), and their importance for synapse elimination (Chung et al.). Many of these functions are also developmentally regulated and thought to contribute to neurodevelopmental disorders (Molofsky et al). However, little is understood about the mechanisms that trigger astrocyte formation and maturation.

Neurons and astrocytes develop from the same progenitor cells in the CNS called radial glia (Malatesta et al.). The “gliogenic switch” is a phenomenon where radial glia transition from a neuronal fate early in gestation to an astrocyte fate at later gestational stages (Miller et al.). The initiation of the gliogenic switch is thought to result from a combination of intrinsic and extrinsic signals sent from neurons back to radial glia (Lanjewar et al.). Experiments involving culturing

of embryonic cortical neural precursors on cortical slices first demonstrated the important impacts of extrinsic signals on astrocyte development. When neural stem cells were cultured on embryonic slices, neurons formed, but when these same cells were cultured on postnatal slices, they attained a predominantly astrogenic fate (Morrow et al.). These experiments demonstrate how signals from neighboring cells in the brain can impact the timing of the gliogenic switch. Some of these extrinsic signals such as LIF, CNTF and BMP4 (Barnabé-Heider et al., Bonni et al.) have been previously identified as important contributors to astrocyte development. LIF and CNTF, act through the heterodimerization of the signal-transducing coreceptors LIFRb and gp130, which act upstream of the Janus kinase/signal transducer and activator of transcription (JAK-STAT) pathway. Mice lacking either LIFRb or gp130 have pronounced deficits in astrogenesis, and gp130−/− or LIFRb−/− NSCs exhibit significantly impaired astrogenesis in vitro (Sloan and Barres, 2014). BMP4 is a primary ligand in the TGF-β signaling network that has been shown to induce astrogenesis through SMAD1 activation and downstream activation of signal transducers and activators of transcription (STATs) (Cole et al., Nakashima et al.). These individual extrinsic signals have been shown to influence astrogenesis on their own, and we understand basic mechanisms of their signaling. However, these signals are never present in isolation in vivo, and it is important to consider the synergistic contributions of these signals together. Thus, this project aims to identify combinations of multiple candidate extrinsic signals that together impact astrocyte development.

To begin, we computationally leveraged gene expression data from the developing brain to identify specific ligand-receptor pairs that contribute to the gliogenic switch and increase astrocyte gene expression and decrease neuronal gene expression. Ligands are common extrinsic signals in the CNS that are secreted by cells to initiate downstream signaling cascades in target

cell populations. Due to this receptor binding specificity, ligands have a unique ability to facilitate cell-cell communication. Given this ability, we aim to identify candidate ligands involved in astrocyte development to further understand extrinsic players in the gliogenic switch.

To identify actively secreted ligands in the developing brain during astrocyte development, we utilized existing bulk and single-cell RNA-Seq data. These cell type-specific datasets allow us to focus on cell populations that are likely to secrete astrogenic ligands (neurons), as well as other progenitor populations that express cognate receptors to these ligands (radial glia) . We leveraged the NicheNet (Browaeys et al.) algorithm, to computationally facilitate the matching of ligands expressed by developing neurons and their cognate receptors expressed on radial glia. Following matching of ligand and receptor pairs, we ranked the pairs based on their likelihood to induce key astrocyte transcriptomic signatures.

We next aimed to experimentally test the candidate ligands at various timepoints throughout astrocyte development. We utilized the human induced pluripotent stem cell (iPSC) derived organoid model system due to its human origins and unique ability to reliably recapitulate the gliogenic switch. Organoids are a stem cell-based model system, so we began experiments by patterning iPSCs with proteins in order to recapitulate dorsal prefrontal cortex development in humans (Sloan et al, 2018). Following patterning, organoids contain a heterogeneous population of neural progenitors, neurons, and developing astrocytes, which resemble the intricate communication networks in the developing fetal brain. A key advantage to this model system is the ease of reproducibility for candidate ligand exposures to organoids at different timepoints throughout development. We can easily differentiate the same line of iPSCs and generate organoids genetically identical to those exposed to ligands in previous experiments.

We exposed cortical organoids to computationally identified candidate ligands for thirty-day periods. Following exposures, we used bulk RNA-Seq to determine ligand effects on the transcriptomic profiles of developing astrocytes. Additionally, we supplemented our findings in the organoid model with primary human fetal tissue ligand exposures and used bulk RNA-Seq and immunohistochemistry to determine ligand-induced morphological changes in astrocyte populations. Our results show that computationally identified neuronal ligands demonstrate synergistic effects on astrocyte development at timepoints immediately preceding and succeeding the gliogenic switch.

Methods

Candidate Ligand Identification

Candidate ligands were identified using the NicheNet (Browaeys et al.) algorithm. The NicheNet pipeline models ligand-receptor pairs and predicts modulation of a set of target genes (described in Figure 1B). Briefly, mouse (Zhang et al.) and human (Eze et al., Fan et al., Polioudakis et al.) RNA-seq data (fastq files) were inputted into the NicheNet algorithm following trimming using Trimmomatic (Bolger et al.), alignment using STAR aligner (Dobin et al), and read summarization using featureCounts (Liao et al.). Following input of transcriptomic data, neurons were defined as the sender cell population and astrocytes, radial glia, or immature astrocytes, if specified, were defined as the receiver cell population. A list of previously identified immature astrocyte genes was used as the gene set of interest to specify targets that might be modulated by ligand-receptor binding (Zhang et al.). Next, we built a ligand-receptor network based on the expressed ligands and receptors in the above datasets. Our final short-list of candidate ligands was then narrowed by ranking a ligand activity list based on the quantity

and breadth of receptors and genes each ligand was predicted to bind to and modulate, respectively.

Generation of cortical organoids

Human cortical organoids were formed from three human induced pluripotent stem cells (iPSC) lines (8858.3, 2242.1 and 1363.1) following a previously published protocol (Pasca et al.). iPSC colonies at 80-90% confluency were detached from culture plates using Accutase and were formed into 3D spheroids using AggreWells. Following 3D formation, spheroids were treated daily in neural induction media supplemented with a BMP inhibitor, Dorsomorphin, and a TGF-β inhibitor, SB-431542, for 6 days. Following this treatment, organoids were treated daily with neural media supplemented with EGF and FGF2 for 10 days, and every other day for days 16-24. At day 25, organoids were treated every other day with neural media supplemented with BDNF and NT-3 to promote differentiation of progenitors. From day 43 onwards, organoids were fed every 3 days with neural media, alone.

Organoid Ligand Exposures

Organoids were exposed to candidate ligands, with media changes every other day, for thirty-day periods between day 45-75, day 60-90, and day 90-120. In preliminary exposures (**Figure 1H, I and 2A, B**), ligands were added in two groups. Group 1 included: APP (20ng/mL, R&D Systems), APOE3 (30ng/mL, Sigma-Aldrich), Gas6 (80ng/mL, R&D Systems), CALR (15ng/mL, abcam), and IGF1 (100ng/mL, Sigma-Aldrich). Group 2 included: TGF-β2 (5ng/mL, R&D Systems), NLGN1 (50ng/mL, Sino Biological, R&D Systems), TSLP (20ng/mL, Sino Biological), DKK1 (20ng/mL, Sigma-Aldrich, R&D Systems), and BMP4 (10ng/mL, Sigma-

Aldrich, R&D Systems). In successive exposures, ligands were added to organoid cultures either in these groups or individually (**Figure 3**).

RNA-Sequencing Library Preparation

Following thirty-day exposures, organoid total RNA was extracted using the miRNeasy kit (Qiagen) under the protocols of the manufacturer. The quality of the RNA was assessed by Bioanalyzer. In preliminary trials (**Figure 1H, I**), the Qiaseq Targeted RNA custom panel (Qiagen) was used to determine the influence of ligands on neuron and astrocyte genes, specifically. In successive trials, bulk RNA-Seq was used to study broad transcriptomic changes. Libraries were created with the NEB Next Ultra II kit with poly-A selection. We obtained 40 million paired-end reads per sample.

RNA-Sequencing Processing and Analysis

Targeted RNA-Seq data was processed using the Qiagen GeneGlobe software and was normalized using DESeq2 (Love et al.). For bulk RNA-Seq, FASTQ files were first trimmed using Trimmomatic and then mapped using STAR aligner. The paired end option was selected, and mouse genome version 10 (mm10) and human genome version 19 (hg19) were used as reference genomes. We then ran FeatureCounts to assemble transcripts and generate raw count matrices. Following determination of raw count data, we used DESeq2 to normalize the data and determine differential gene expression.

Immunopanning organoid-derived and fetal human astrocytes

Astrocytes were purified from human fetal tissue aged between 17-20 gestational weeks. The tissue was chopped using a #10 blade and then incubated in 30 U/ml papain at 34°C for 90 minutes and washed with a protease inhibitor solution (ovomucoid). After digestion, the tissue was triturated and then the resulting single-cell suspension was added to a series of plastic petri dish pre-coated with cell type specific antibodies and incubated for 10–30 minutes each at room temperature. Unbound cells were transferred to the subsequent petri dish while the dish with bound cells was rinsed with PBS to wash away loosely bound contaminating cell types. The antibodies used include anti-CD45 to harvest and deplete microglia/macrophages, anti–Thy1 to harvest and deplete neurons, and anti–CD49f to harvest astrocytes. For RNA-seq, cell samples were scraped off the panning dish directly with Qiazol reagent (Qiagen). For cell culture and in vitro experiments, astrocytes bound to the antibody coated dishes were incubated in a trypsin solution at 37°C for 3–5 minutes and gently squirted off the plate. We then spun down the cells and plated them on poly-D-lysine coated plastic coverslips in a Neurobasal/DMEM based serum-free medium. We replaced the media every other day to maintain the cultures for a total of 12 days.

For immunopanning of organoids (**Figure 2**), the same protocol described above was used with minimal exceptions. Organoids were collected at 10-day intervals from day 70 through day 110 and immunopanned with anti-HepaCAM antibody. Pulldown of at least 10,000 cells (~5% yield) was the threshold used to determine “success” of the gliogenic switch in each sample.

Immunocytochemistry

Cultured cells were fixed with 4% PFA for 10 minutes at room temperature, permeabilized and blocked with 10% donkey serum with 0.2% Triton-X100. Antibodies used were GFAP (DAKO, Z0334, dilution 1:1500) and Ki67(BD, b550609, dilution 1:50). We also used modified thymidine analogue EdU (Invitrogen) to measure proliferation.

Astrocyte Morphology Quantification

Images of GFAP+ cells were traced and analyzed using the Fiji plug-in SNT. 20 cells from the control and candidate ligand exposed conditions were traced using SNT's semi-automated tracing method. Primary branches originate at the nucleus. Secondary branches extend off of primary branches, and tertiary branches extend off of secondary branches. The SNT software quantified the total path number, primary, secondary, and tertiary path numbers, and path length for each cell.

Immunohistochemistry

Organoids were fixed with 4% PFA for 30 minutes at room temperature, rinsed with PBS, and then equilibrated with 30% sucrose overnight. After organoids sunk to the bottom of the tube, they were embedded in OCT blocks and frozen for cryosectioning (12um sections). Sections were mounted on glass slides, permeabilized, and blocked with 10% donkey serum with 0.2% Triton-X100. Antibodies used included GFAP (DAKO, Z0334, dilution 1:1500).

qPCR

The primers used in this study are listed below:

GFAP Forward: GAGAACCGGATCACCATTCC

GFAP Reverse: CCCAGTCTGGAGCAACCTAC

GAPDH Forward: AATCCCATCACCATCTTCCA

GAPDH Reverse: TGGACTCCACGACGTACTCA

We performed 40 cycles of amplification for all samples. The specificity and efficiency of all primers were first validated using gel electrophoresis and qPCR with serial dilutions. The determination of each gene's CT in qPCR was performed in triplicate. When determining fold changes in gene expression across samples, the CT of each gene was normalized according to the CT of the housekeeping gene in the same sample.

Results

NicheNet predicts ligand and receptor pairs that influence astrocyte development

In humans, neurogenesis begins between approximately 6-8 gestational weeks. This temporally precedes gliogenesis, which starts between 16-18 gestational weeks (Lanjewar et al.). While we know that neurons and astrocytes share the same progenitor cell called radial glia, it is unclear which extrinsic ligands are sufficient to influence the cell fate switch in these progenitors from neurogenesis to gliogenesis (**Figure 1A**). To identify candidate ligands that promote astrocyte development, we applied an algorithm called NicheNet (Browaeys et al.) to bulk and single-cell RNA-Seq data from mouse and human samples. NicheNet is a powerful tool for

candidate ligand identification because it outputs both probable ligand and receptor pairs and the likelihood of ligand/receptor interactions modulating a predefined list of downstream genes.

We began by applying mouse bulk RNA-Seq data (Zhang et al.) into the NicheNet pipeline, and we identified 5 candidate ligands that were (1) expressed in neurons, (2) had cognate receptor expression in radial glia, and (3) had ligand-receptor interactions thought to modulate expression of astrocyte genes: Amyloid Precursor Protein (APP), Apolipoprotein E (APOE), Insulin Like Growth Factor I (IGF1), Calreticulin (CALR), and Growth Arrest Specific 6 (GAS6). We chose these candidates based on their differential binding to cognate receptors on radial glia and predicted modulation of different and complimentary astrocyte genes (**Figure 1D**). Additionally, we prioritized candidates, such as BMP4, that have previously been shown to be involved in neurodevelopment or signaling pathways that are implicated in neurodevelopment (Cole et al.).

Following identification of mouse-derived ligands, we next focused on using human single-cell RNA-Seq data to identify human-derived candidate ligands. Mouse RNA-Seq data provided an excellent starting point to study deeply sequenced, cell type specific data in the developing brain. Another alternative is to use human data, which is largely limited to single-cell RNA-Seq at the early developmental timepoints when gliogenesis occurs. In addition, single-cell transcriptomic data is beneficial because it provides cell type specificity, but a major tradeoff is decreased sequencing depth.

Following input of human single-cell RNA-Seq data from early and mid-gestational timepoints into the NicheNet pipeline, we found little overlap between candidate ligands identified from the mouse and human datasets. From the human single-cell data, we identified: Dickkopf-1 (DKK1), Bone Morphogenetic Protein 4 (BMP4), Neuroligin 1 (NLGN1),

Transforming Growth Factor Beta 2 (TGF-β2), and Thymic Stromal Lymphopoietin (TSLP). Notably, these candidates primarily modulate a set of downstream genes, that are different from those modulated by the candidate mouse-derived ligands (**Figure 1F**).

Targeted RNA-Sequencing reveals increased astrocyte signature following ligand exposures

We next wanted to test whether the candidate neuronally-secreted ligands could impact astrocyte development in vitro. Therefore, we generated iPSC organoids from 3 separate lines (2242.1, 1363.1, and 8858.3) and performed exposures using three different ligand conditions: We exposed all ten candidate ligands together, ligands 1-5 together, and ligands 6-10 together every other day for thirty days. As a readout of whether astrocyte development was affected, we used a custom-designed targeted RNA-Seq panel that includes 40 astrocyte genes, 40 neuronal genes, 10 reactive genes, and 10 control genes (**Figure 1G**). We included reactive and control genes on the panel to determine if the addition of ligands made organoid cultures reactive or impacted normal housekeeping cell functions.

Following a 30-day exposure of the ten candidate ligands between day 60-90, we harvested RNA and prepared libraries for targeted RNA-Seq. From this panel, differential gene expression analysis via EdgeR (Robinson et al.) revealed a consistent upregulation of astrocyte genes and downregulation of neuronal genes while reactive and control genes did not significantly change (**Figure 1H-I**).

Bulk RNA-Sequencing confirms upregulation of astrocyte genes and downregulation of neuron genes

Given the preliminary evidence for ligand-induced upregulation of astrocyte genes demonstrated by targeted RNA-Seq, we next utilized bulk RNA-Seq to identify ligand-induced transcriptomic changes throughout the genome at the day 60-90 timepoint. We established cell type specific signatures from a group of 25 astrocyte-specific and 25 neuronal-specific genes (Zhang et al.) to gauge potential influences on astrocyte and/or neuronal developmental trajectories. Using a large panel of genes helps ensure that our interpretation is not biased by the specific induction of a small subset of marker genes upon addition of candidate ligands. Bulk RNA-Seq differential gene expression analysis revealed no significant difference (Mann Whitney-U, $p = .538$) between neuron and astrocyte gene expression levels when organoids were exposed to APP, APOE, CALR, GAS6, and IGF1 (Ligands 1-5). However, bulk RNA-Seq of organoids exposed to TGF-β2, NLGN1, TSLP, DKK1, and BMP4 (Ligands 6-10) showed a significant (Mann Whitney U, $p = .002$) upregulation of astrocyte genes and downregulation of neuronal genes compared to controls (**Figure 2B, C**). In what follows, candidate ligands will exclusively refer to ligands 6-10.

The gliogenic switch occurs between organoid day 70-110

Throughout development, the expression of many of the NicheNet predicted receptors within radial glia changes. Thus, it is important to consider how ligand binding might differ at specific timepoints when these receptors are more or less abundant. To determine the temporal windows when the candidate ligands are most potent, we needed to first establish the precise timing of the gliogenic switch within human cortical organoids.

Based on previous studies (Miller and Gauthier), we estimated that the gliogenic switch occurs roughly between day 70-110 in organoids. Therefore, we sought to systematically quantify the precise timing of the gliogenic switch. We used three separate metrics to define the onset of gliogenesis (IHC, qPCR, and immunopanning) and performed these assays on organoids collected every 10 days, starting at day 70 and extending through day 110.

To quantify GFAP expression, we fixed organoids and immunustained for GFAP. We then quantified the percentage of GFAP positive cells (as a % of DAPI+ cells) in Fiji and considered gliogenesis initiated if the GFAP+ percentage exceeded 5% of total cells. To quantify GFAP mRNA expression, we harvested RNA from the entire organoid and considered the onset of gliogenesis when the qPCR CT threshold reached below 30 cycles (defined because GFAP CT values fall below 30 during the initiation of gliogenesis (16-18 GW) in human fetal samples).

In addition to quantifying GFAP as a metric of gliogenesis, we purified HepaCAM+ astrocytes from organoids via immunopanning. Following immunopanning, we counted cells that were bound to the panning plate and used a threshold of greater than or equal to 10,000 cells as evidence of the initiation gliogenic switch.

All three methodologies (IHC, qPCR and immunopanning) converged on an onset of astrogenesis between organoid day 90-100 (**Figure 2E-G**).

Ligand exposures affects astrocyte development before and after the gliogenic switch

Based on this timeline of astrogenesis, we focused on exposure timepoints far preceding day 90 (day 45-75), immediately before day 90 (day 60-90) and immediately after day 90 (day 90-120). These timepoints allow us to determine the ligands' developmental effects and parse out whether the synergistic effects of the ligands primarily affect astrogenesis or begin to influence

maturation. At these three key developmental intervals, we exposed organoid cultures to candidate ligands every other day. During exposures that lasted from day 45-75, we found no significant difference (Mann Whitney U, $p = .643$) between astrocyte and neuronal gene expression. However, at the day 60-90 and day 90-120 exposures, we observed a significant increase in astrocyte genes and concomitant decrease in neuronal genes expression (Mann Whitney U, $p \leq .0001$ at each timepoint) (**Figure 2H, I**).

Given this change in astrocyte and neuronal gene expression specifically at timepoints surrounding the gliogenic switch, we predicted that the expression patterns of our receptors of interest might correlate with developmental stages when the ligands had the most impact. To test this hypothesis, we analyzed the expression of the receptors predicted to bind to the candidate ligands throughout astrocyte development at various developmental timepoints using bulk RNA-Seq data (day 35, day 50, day 75, day 110) (**Figure 1D, E, F**). We found that the majority of the predicted ligand-binding receptors increase expression as organoids age (**Figure 2J, K**). Thus, the lack of significant changes in astrocyte and neuronal gene expression following ligand exposures from day 45-75, could be the result of decreased expression of receptors on radial glia at these timepoints. These data further confirm that the day 60-90 and day 90-120 exposures fall within a key period for astrocyte development.

Ligands work synergistically, but not individually, to influence astrocyte development

Given the data supporting changes in astrocyte development following a concomitant five-ligand exposure during the day 60-90 and day 90-120 timepoints, we next sought to understand the impacts of individual ligands on astrocyte development. We performed 2 varieties of ligand exposures from day 60-90 and day 90-120. The first followed the paradigm in **Figure**

2, adding a cocktail of candidate ligands. In the second, we added each ligand individually to organoid cultures. Of the ligands added individually, only BMP4 showed a significant increase in astrocyte gene signatures and significant decrease in neuron gene signatures. We observed in each condition that the degree of astrocyte signature induction was always greatest with all 5 ligands combined (**Figure 3B, E**). Additionally, the degree of neuronal signatures decreased significantly when all 5 ligands were combined rather than added individually (**Figure 3C, F**).

Purified fetal astrocytes validate astrocyte development in ligand-exposed organoids

With evidence of transcriptomic changes in organoid astrocyte populations, we next aimed to benchmark the organoid model against primary human astrocytes. We purified CD49f+ astrocyte populations from fetal human brain tissue between 17-20 gestational weeks collected by immunopanning. Following purification, astrocytes were cultured for 10-12 days with ligand exposures occurring every other day. Following culture, bulk RNA-Seq revealed similar patterns to organoids in both astrocyte and neuron transcriptomic signatures. In both sample types and across replicates we see an increased number of upregulated differentially expressed genes (DEGs) compared to downregulated DEGs. Both samples demonstrated significant upregulation of astrocyte markers such as CRYAB and AQP4 and significant downregulation of neuron markers such as EOMES and SNAP25 (**Figure 4D**).

Ligands drive mature astrocyte morphology in purified fetal astrocytes

With evidence for transcriptomic changes in human fetal astrocytes following ligand exposures, we next aimed to understand the effects of candidate ligands on astrocyte morphology. Studying morphology allowed us to quantify the effects of the ligands on astrocyte structure, which can be a useful indicator of astrocyte maturation. Radial glia typically have a bipolar morphology while mature astrocytes have a more branched, star-shaped morphology (Kriegstein et al.).

Purified cd49f+ fetal cells (between 17-20 gestational weeks) were cultured for 10-12 days, and ligands were added every other day. We then fixed these ligand-exposed purified fetal astrocyte cultures and utilized IHC to immunostain for GFAP (**Figure 4A**). Using the SNT plugin in Fiji, we quantified GFAP+ cells through a semi-automated tracing of astrocyte processes. Primary branches are defined as the branches directly extending from the nucleus of the cell, secondary branches extend off of the primary branches, and tertiary branches extend off of secondary branches. SNT provides an output of branch length and number of primary, secondary, and tertiary branches. Additionally, we quantified boundary size/area of each cell. Using this output, we found a significantly increased number of total branches (Mann-Whitney U test, **$p<.001$), significantly increased number of secondary branches (Mann-Whitney U test, *$p<.05$), significantly decreased branch length (Mann-Whitney U test, ***$p<.0001$), and significantly decreased boundary size (Mann-Whitney U test, ***$p<.0001$) compared to control GFAP stains in ligand-exposed astrocyte cultures, indicative of a more mature state (Bushong et al.) (**Figure 4B, C**).

Discussion

Here we show the synergistic contributions of computationally-predicted ligands on astrocyte development. Specially, we show that TGF-β2, NLGN1, TSLP, DKK1, and BMP4 can work synergistically to initiate early astrogenesis from day 60-90 and accelerate astrocyte maturation from day 90-120. Additionally, we validate the organoid exposure paradigm through the use of purified fetal astrocytes and show astrocyte morphological changes following fetal astrocyte ligand exposures.

Notably, this study is the first to apply computational methods to identify ligand and receptor pairs that drive astrocyte maturation. By applying NicheNet to developmental brain RNA-Seq data and testing candidate ligands in the organoid model, we both validated the NicheNet paradigm and its applications for neurodevelopment, and demonstrated the impact of the predicted ligands at specific timepoints throughout astrocyte development.

Additionally, these data provide increased insight into how neurons interact and communicate with glia, and specifically astrocytes. Specifying neurons as sender cells in NicheNet allowed us to exclusively focus on neuronally expressed ligands. This cell-type specificity of both sender and receiving cell, is crucial to a deeper understanding of the pathways and communication in the developing brain.

While we chose to focus on neurons based on their solidified developmental presence prior to the gliogenic switch, making them a likely candidate to regulate the development of other cell types, we recognize that other cell types present during development might also express influential ligands for astrocyte development. Specifically, it would be interesting to further explore the influence of microglia, which are also present in the developing CNS prior to astrogenesis, on astrocyte development (Ginhoux et al.).

Our results demonstrate the impact of synergistic contributions of extrinsic signals on astrocyte development. After adding ligands individually, we observed no significant change in astrocyte gene expression, with the exception of BMP4. Numerous studies have shown the involvement of specifically BMP4 on astrocyte development (Cole et al., Gomes et al.). These studies include paradigms, such as ours, in which BMP4 is added exogenously. While we observed significant changes to astrocyte and neuron development when BMP4 was added alone, exposing organoids to the candidate ligand cocktail showed a significant increase in astrocyte gene expression compared to when BMP4 alone was added. Given this, we hypothesize that BMP4 acts in combination with other pathways to influence downstream astrocyte genes. For example, the timing of astrocyte maturation might depend on high expression of both BMP4 (a TGF-β pathway activator) and DKK1 (a WNT pathway agonist). Our results indicate that the effects of BMP4 in isolation do not fully encompass the potential extrinsic influences on astrocyte development, and future studies could help us further understand the specific interaction of BMP4 with key developmental pathways.

Additionally, these data will be influential for inducing early astrogenesis in organoid or other *in vitro* cultures. Astrogenesis occurs between day 90 and day 100 in organoids. However, addition of candidate ligands could expediate the process of astrocyte development by allowing us to study impacts of accelerated astrocyte development on other cell types, such as neurons. Studying expedited astrogenesis and astrocyte maturation could greatly aid in our understanding of neurodevelopmental disorders such as autism and schizophrenia, where the timing of astrocyte development is often disrupted. If candidate ligands are highly expressed and astrogenesis occurs earlier than the typical 16-18 gestational week range, then this could end neurogenesis

prematurely and ultimately lead to symptoms of these neurodevelopmental disorders as a result of abnormal circuit development.

Ongoing Experiments

In late March 2022, we have ongoing projects to provide additional insight into the ligand-induced astrocyte developmental changes. We are currently culturing purified fetal CD49f+ astrocytes with ligands in the presence of EDU to test whether ligand exposure leads to changes in proliferation. Based on our previous transcriptomic and morphological results, we expect a decreased quantity of EDU+ cells in ligand-exposed conditions compared to controls, indicative of a more mature, quiescent profile. We are also validating our existing bulk RNA-Seq results with single-cell RNA-Seq in order to obtain cell-type specific evidence of the neuronal and astrocyte changes, rather than the global values obtained from bulk RNA-Seq on entire organoids. This will also allow us to further pinpoint differences in astrocyte-specific populations since we can look at expression changes in that population specifically. Additionally, we are running a pathway phosphorylation analysis (BioRad) to determine how ligand exposure influences activation of the TGF-β, NFkB, AKT, MAPK, and JAK/STAT pathways at the protein level.

Future Directions

This study demonstrated the impact of neuronal ligands known to be involved in various developmental pathways related to astrocyte development. However, it is also important to consider the impact of ligands secreted by other cell types present preceding and simultaneously forming during the gliogenic switch, such as microglia and oligodendrocyte precursor cells. Computationally analyzing and testing ligands secreted by these cells, in addition to neurons, will allow us to develop a more complete understanding of the synergistic effects of extracellular communication on development.

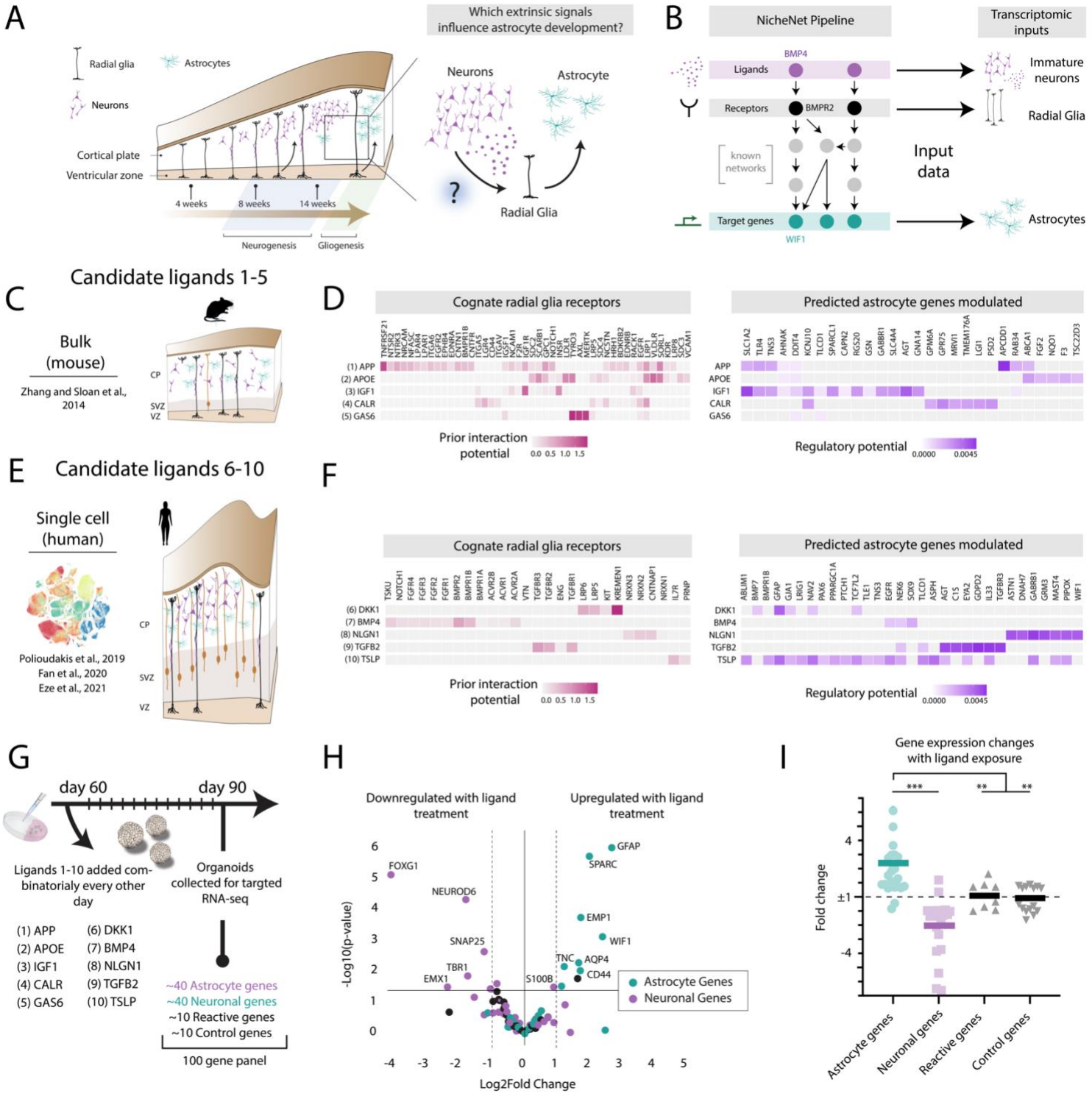
A
Which extrinsic signals influence astrocyte development?
Radial glia
Astrocytes
Neurons
Cortical plate
Ventricular zone
4 weeks
8 weeks
14 weeks
Neurogenesis
Gliogenesis
Neurons
Astrocyte
?
Radial Glia
B
NicheNet Pipeline
Transcriptomic inputs
BMP4
Ligands
Receptors
BMPR2
known networks
Input data
Target genes
WIF1
Immature neurons
Radial Glia
Astrocytes
C
Candidate ligands 1-5
Bulk (mouse)
Zhang and Sloan et al., 2014
CP
SVZ
VZ
D
Cognate radial glia receptors
Predicted astrocyte genes modulated
(1) APP
(2) APOE
(3) IGF1
(4) CALR
(5) GAS6
Prior interaction potential
0.0 0.5 1.0 1.5
Regulatory potential
0.0000
0.0045
E
Candidate ligands 6-10
Single cell (human)
Polioudakis et al., 2019
Fan et al., 2020
Eze et al., 2021
CP
SVZ
VZ
F
Cognate radial glia receptors
Predicted astrocyte genes modulated
(6) DKK1
(7) BMP4
(8) NLGN1
(9) TGFB2
(10) TSLP
Prior interaction potential
0.0 0.5 1.0 1.5
Regulatory potential
0.0000
0.0045
G
day 60
day 90
Ligands 1-10 added combinatorialy every other day
Organoids collected for targted RNA-seq
(1) APP
(2) APOE
(3) IGF1
(4) CALR
(5) GAS6
(6) DKK1
(7) BMP4
(8) NLGN1
(9) TGFB2
(10) TSLP
~40 Astrocyte genes
~40 Neuronal genes
~10 Reactive genes
~10 Control genes
100 gene panel
H
Downregulated with ligand treatment
Upregulated with ligand treatment
FOXG1
NEUROD6
SNAP25
TBR1
EMX1
GFAP
SPARC
EMP1
WIF1
AQP4
CD44
TNC
S100B
Astrocyte Genes
Neuronal Genes
-Log10(p-value)
Log2Fold Change
I
Gene expression changes with ligand exposure
***
**
**
Fold change
±1
Astrocyte genes
Neuronal genes
Reactive genes
Control genes

Figure 1. Determining candidate neuronal ligands and measuring their effect on astrocyte development. **A.** Schematic depicting the timing of neurogenesis and gliogenesis and how neurons secrete ligands that ultimately influence astrocyte maturation. Neurogenesis precedes gliogenesis and generally occurs approximately between gestational weeks 8-14. **B.** Schematic of the NicheNet pipeline. Ligands and receptor pairs are connected based on previous knowledge of ligand pathway involvement, and a likelihood score for astrocyte target gene modulation is outputted for each pair. **C.** Schematic of mouse, bulk RNA-Seq data cell type locations used to generate candidate ligands 1-5. **D.** NicheNet heatmap outputs depicting the potential for ligands 1-5 to bind to cognate radial glia receptors and the potential for ligands 1-5 to regulate downstream astrocyte genes. **E.** Schematic of human, single-cell RNA-Seq data cell type locations used to generate candidate ligands 6-10. **F.** NicheNet heatmap outputs depicting the potential for ligands 6-10 to bind to cognate radial glia receptors and the potential for ligands 6-10 to regulate downstream astrocyte genes. **G.** Schematic of ligand exposure paradigm with a targeted RNA-Seq readout. Ligands were added to organoid cultures every other day between organoid day 60-90. At day 90, RNA was extracted for targeted RNA-Seq. The Targeted RNA-Seq panel included 40 astrocyte genes, 40 neuron genes, 10 reactive genes, and 10 control genes. **H.** Volcano plot of targeted RNA-Seq data from day 60-90 ligand exposures depicting upregulation of astrocyte genes and downregulation of neuron genes. **I.** Mann-Whitney U test reveals significantly increased astrocyte gene expression and significantly decreased neuron gene expression following day 60-90 ligand exposures (*** $p<.001$, ** $p<.01$).

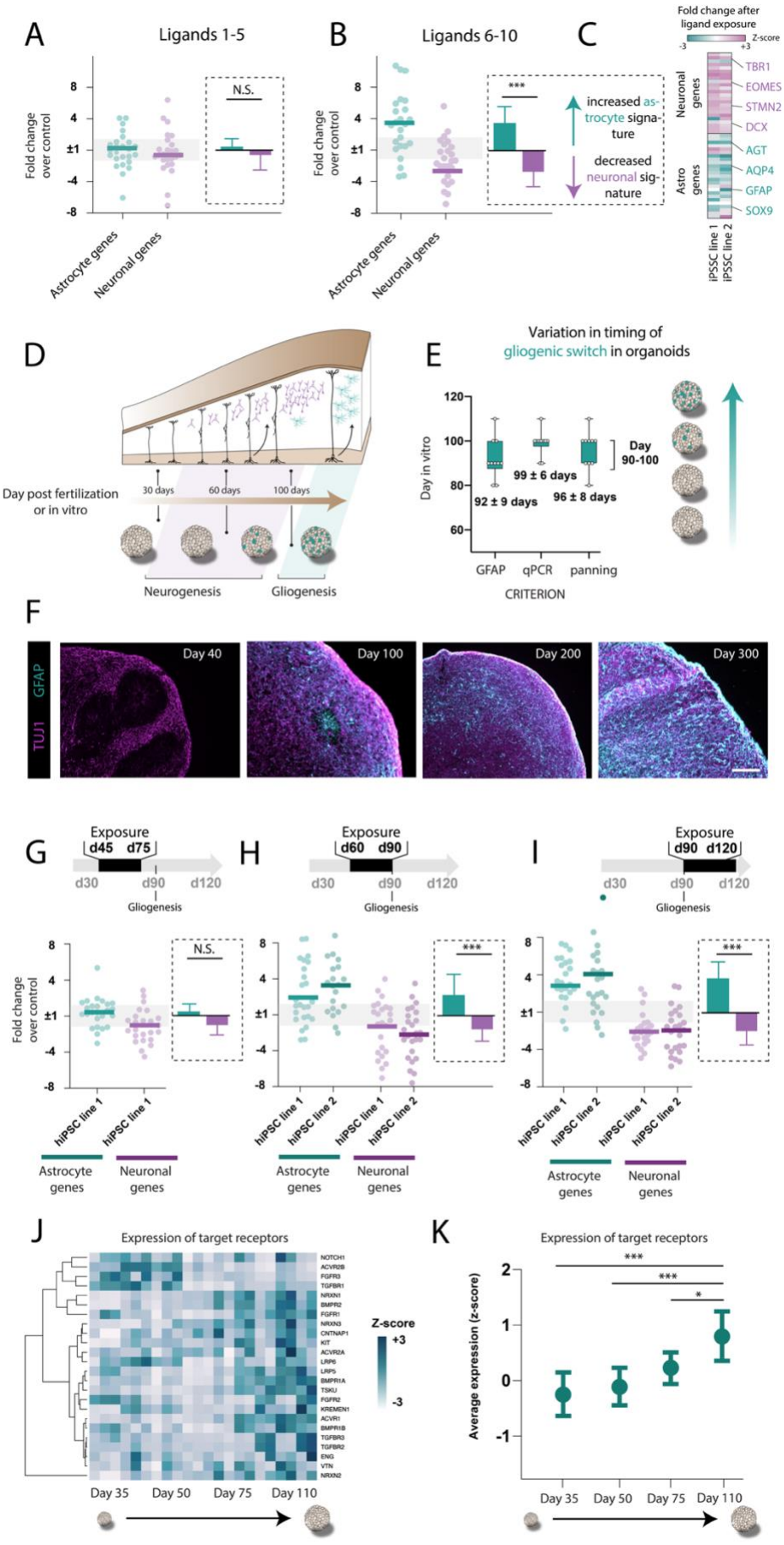
A
Ligands 1-5
Fold change over control
N.S.
Astrocyte genes
Neuronal genes
B
Ligands 6-10
***
C
Fold change after ligand exposure
Z-score
increased astrocyte signature
decreased neuronal signature
Neuronal genes
Astro genes
TBR1
EOMES
STMN2
DCX
AGT
AQP4
GFAP
SOX9
iPSSC line 1
iPSSC line 2
D
Day post fertilization or in vitro
30 days
60 days
100 days
Neurogenesis
Gliogenesis
E
Variation in timing of gliogenic switch in organoids
Day in vitro
92 ± 9 days
99 ± 6 days
96 ± 8 days
Day 90-100
GFAP
qPCR
panning
CRITERION
F
TUJ1
GFAP
Day 40
Day 100
Day 200
Day 300
G
Exposure
d45 d75
d30
d90
d120
Gliogenesis
N.S.
hiPSC line 1
Astrocyte genes
Neuronal genes
H
Exposure
d60 d90
***
hiPSC line 2
I
Exposure
d90 d120
J
Expression of target receptors
Z-score
Day 35
Day 50
Day 75
Day 110
K
Expression of target receptors
Average expression (z-score)

Figure 2. Organoid ligand exposures at crucial developmental intervals. **A.** Ligands 1-5 exposed organoids have astrocyte and neuron gene expression values that do not change significantly compared to control organoids. **B.** Ligands 6-10 exposed organoids have an increased astrocyte signature and decreased neuron signature compared to control organoids (***p < .0001). **C.** Heatmap of neuronal and astrocyte gene expression following ligand exposure. Signature genes for each population are highlighted. **D.** Schematic of timeline of the gliogenic switch in organoid cultures. **E.** Determining the timing of the gliogenic switch. Organoids were fixed, purified, or RNA extracted at every 10 days between day 60-120. After fixation, organoids were stained for GFAP, and if organoids met a threshold of ≥ 5% then the age of the organoid was marked as a gliogenic switch timepoint. GFAP gene expression was quantified via qPCR using a threshold cutoff of CT = 30. HepaCAM+ organoid astrocytes were purified via immunopanning. If there are ≥ 10,000 cells per plate, then the age of organoid astrocytes is marked as a gliogenic switch timepoint. F. GFAP and TUJ1 staining of day 40, day 100, day 200, and day 300 organoids. Scale bar =100 μm, **H.** Organoid ligand 6-10 exposures at the beginning of neurogenesis (day 45-75), preceding the gliogenic switch (day 60-90), and succeeding the gliogenic switch (day 90-120). **G.** No significant change was seen astrocyte and neuron gene expression following day 45-75 exposures. **H-I.** A significant increase in astrocyte gene expression and a significant decrease in neuron gene expression was seen in day 60-90 and day 90-120 exposures (***p<.0001, ***p<.0001). **J-K.** Expression of predicted NicheNet target receptors significantly increases between organoid d35-d110 (***p<.0001, ***p<.0001, *p = .013).

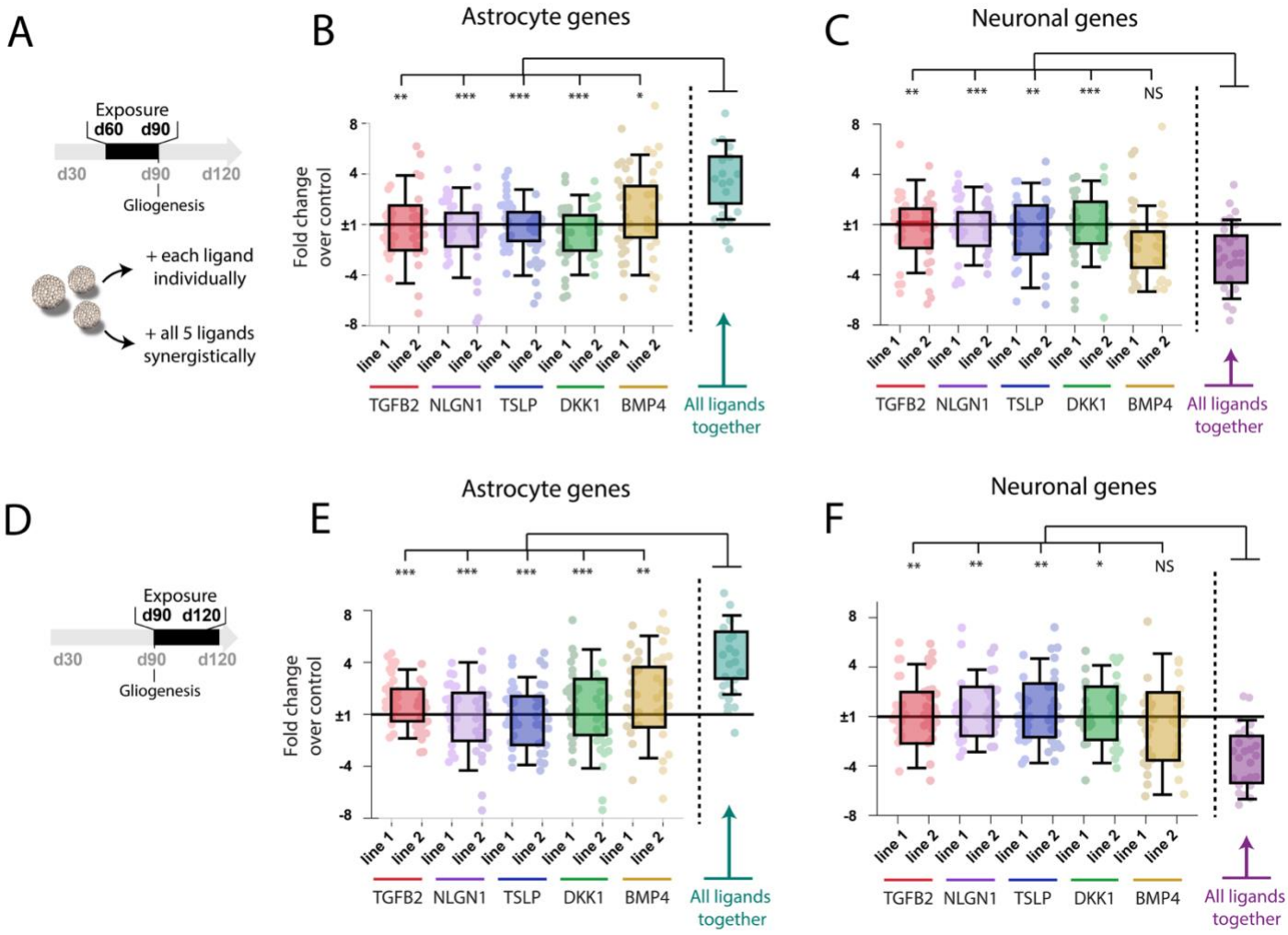
A
Exposure
d60 d90
d30
d90
d120
Gliogenesis
+ each ligand individually
+ all 5 ligands synergistically
B
Astrocyte genes
Fold change over control
line 1
line 2
TGFB2
NLGN1
TSLP
DKK1
BMP4
All ligands together
C
Neuronal genes
NS
D
Exposure
d90 d120
E
F

Figure 3. Synergistic and individual contributions of ligands 6-10. **A.** Schematic of individual ligand exposure paradigm. Ligands were added every other day between day 60-90 either in wells individually or combined together in a cocktail. **B.** Astrocyte gene signatures significantly increase when ligands were added together compared to effects when ligands were added individually. **C.** Neuron gene signatures significantly decrease when ligands were added together compared to ligands were added together compared to effects when ligands were added individually, with the exception of BMP4. **D.** Schematic of individual ligand exposure paradigm. Ligands were added every other day between day 90-120 both in wells individually and together in a cocktail. **E.** Astrocyte gene signatures significantly increase when ligands were added together ligands were added together compared to effects when ligands were added individually. **F.** Neuron gene signatures significantly decrease when ligands were added together compared to effects when ligands were added individually, with the exception of BMP4. *** $p<.0001$, **$p<.001$, *$p<.01$

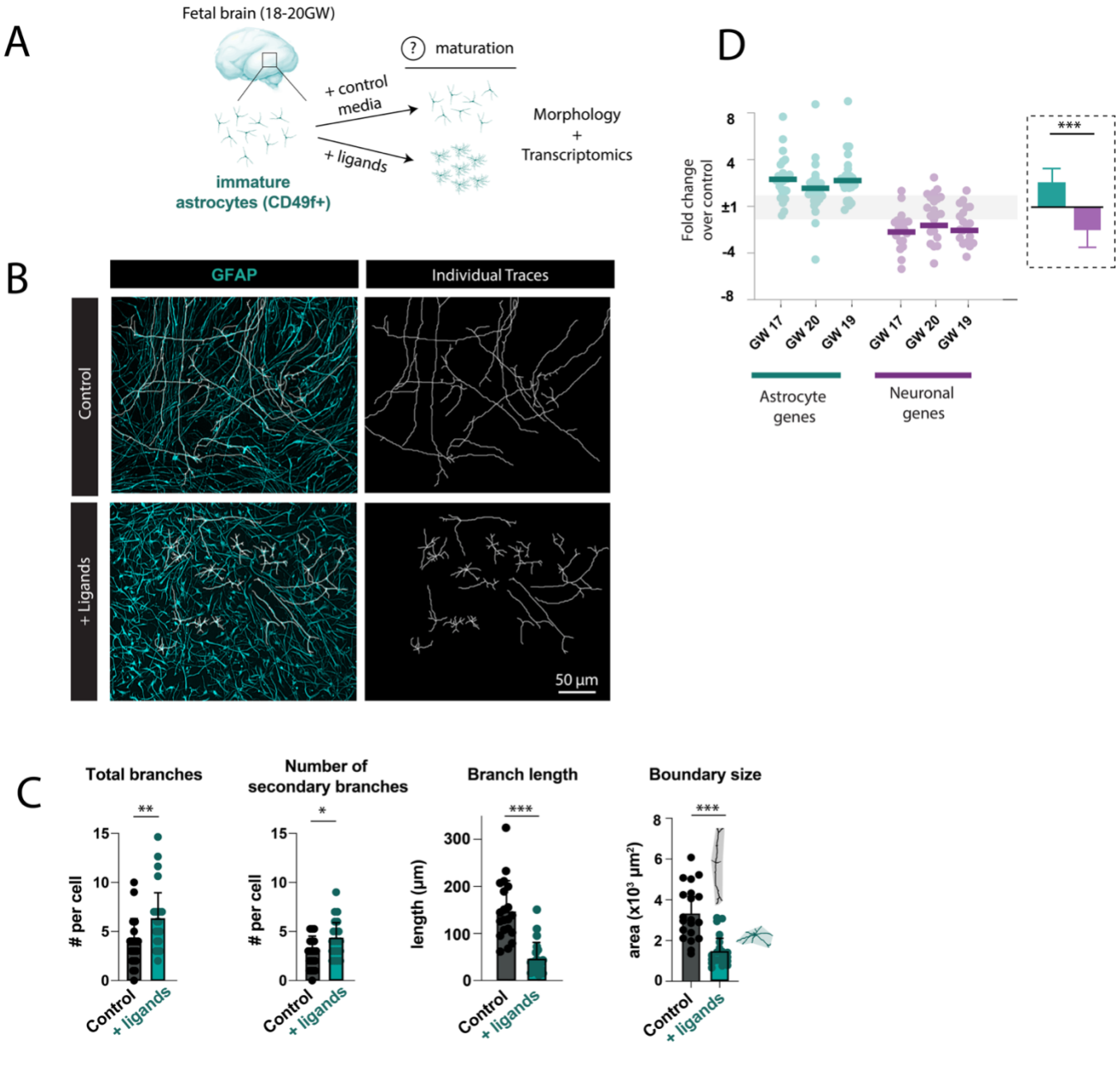
A
Fetal brain (18-20GW)
? maturation
+ control media
+ ligands
Morphology + Transcriptomics
immature astrocytes (CD49f+)
B
GFAP
Individual Traces
Control
+ Ligands
50 µm
C
Total branches
Number of secondary branches
Branch length
Boundary size
per cell
length (µm)
area (x10³ µm²)
Control
+ ligands
D
Fold change over control
GW 17
GW 20
GW 19
Astrocyte genes
Neuronal genes
***

Figure 4. Impact of candidate ligand exposures on fetal tissue gene signatures and morphology. **A.** Schematic of fetal tissue purification and ligand exposure paradigm. Fetal tissue was first immunopanned for CD49f, cultured for 10-12 days with ligand exposures every other day. Following culture, cells were fixed for IHC or RNA extracted for bulk RNA-Seq. **B.** GFAP+ cell process traces from ligand-exposed and control CD49f+ fetal cells. Scale bar = 50 μm. **C.** GFAP+ cell process quantification. Primary branches extend from the nucleus. Secondary branches extend from primary branches. Total branches is the number of processes extending from both the nucleus and primary branches. Boundary size is the area (x 10^3 μm^2) of the image field that one cell occupies. Ligand exposed CD49f processes have an increased number of total branches (**p<.001), increased number of secondary branches (*p<.01), decreased branch length (***p<.0001), and decreased boundary size (***p<.0001) compared to control CD49f cells. **D.** Purified CD49f+ fetal cell bulk RNA-Seq. Astrocyte gene signature significantly increases compared to control while neuron gene signature significantly decreases compared to control in ligand exposed samples.

References

Baldwin KT, Eroglu C (2017) Molecular mechanisms of astrocyte-induced synaptogenesis. Curr Opin Neurobiol 45:113–120.

Barnabé-Heider F, Wasylnka JA, Fernandes KJL, Porsche C, Sendtner M, Kaplan DR, Miller FD (2005) Evidence that embryonic neurons regulate the onset of cortical gliogenesis via cardiotrophin-1. Neuron 48:253–265.

Bonni A, Sun Y, Nadal-Vicens M, Bhatt A, Frank DA, Rozovsky I, Stahl N, Yancopoulos GD, Greenberg ME (1997) Regulation of gliogenesis in the central nervous system by the JAK-STAT signaling pathway. Science 278:477–483.

Browaeys R, Saelens W, Saeys Y (2020) NicheNet: modeling intercellular communication by linking ligands to target genes. Nat Methods 17:159–162.

Bushong EA, Martone ME, Ellisman MH (2004) Maturation of astrocyte morphology and the establishment of astrocyte domains during postnatal hippocampal development. Int J Dev Neurosci 22:73–86.

Chung W-S, Clarke LE, Wang GX, Stafford BK, Sher A, Chakraborty C, Joung J, Foo LC, Thompson A, Chen C, Smith SJ, Barres BA (2013) Astrocytes mediate synapse elimination through MEGF10 and MERTK pathways. Nature 504:394–400.

Cole AE, Murray SS, Xiao J (2016) Bone Morphogenetic Protein 4 Signalling in Neural Stem and Progenitor Cells during Development and after Injury. Stem Cells Int 2016:9260592.

Eze UC, Bhaduri A, Haeussler M, Nowakowski TJ, Kriegstein AR (2021) Single-cell atlas of early human brain development highlights heterogeneity of human neuroepithelial cells and early radial glia. Nat Neurosci 24:584–594.

Fan X, Dong J, Zhong S, Wei Y, Wu Q, Yan L, Yong J, Sun L, Wang X, Zhao Y, Wang W, Yan J, Wang X, Qiao J, Tang F (2018) Spatial transcriptomic survey of human embryonic cerebral cortex by single-cell RNA-seq analysis. Cell Res 28:730–745.

Ginhoux F, Lim S, Hoeffel G, Low D, Huber T (2013) Origin and differentiation of microglia. Front Cell Neurosci 7:45.

Gomes WA, Mehler MF, Kessler JA (2003) Transgenic overexpression of BMP4 increases astroglial and decreases oligodendroglial lineage commitment. Developmental Biology 255:164–177.

Kim YS, Choi J, Yoon B-E (2020) Neuron-Glia Interactions in Neurodevelopmental Disorders. Cells 9:E2176.

Kriegstein A, Alvarez-Buylla A (2009) The Glial Nature of Embryonic and Adult Neural Stem Cells. Annu Rev Neurosci 32:149–184.

Kubotera H, Ikeshima-Kataoka H, Hatashita Y, Allegra Mascaro AL, Pavone FS, Inoue T (2019) Astrocytic endfeet re-cover blood vessels after removal by laser ablation. Sci Rep 9:1263.

Lanjewar SN, Sloan SA (2021) Growing Glia: Cultivating Human Stem Cell Models of Gliogenesis in Health and Disease. Frontiers in Cell and Developmental Biology 9 Available at: https://www.frontiersin.org/article/10.3389/fcell.2021.649538 [Accessed March 14, 2022].

Liao Y, Smyth GK, Shi W (2014) featureCounts: an efficient general purpose program for assigning sequence reads to genomic features. Bioinformatics 30:923–930.

Love MI, Huber W, Anders S (2014) Moderated estimation of fold change and dispersion for RNA-seq data with DESeq2. Genome Biology 15:550.

Malatesta P, Hartfuss E, Götz M (2000) Isolation of radial glial cells by fluorescent-activated cell sorting reveals a neuronal lineage. Development 127:5253–5263.

Miller CA, Sweatt JD (2007) Covalent modification of DNA regulates memory formation. Neuron 53:857–869.

Miller FD, Gauthier AS (2007) Timing Is Everything: Making Neurons versus Glia in the Developing Cortex. Neuron 54:357–369.

Molofsky AV, Deneen B (2015) Astrocyte development: A Guide for the Perplexed. Glia 63:1320–1329.

Molofsky AV, Krenick R, Ullian E, Tsai H, Deneen B, Richardson WD, Barres BA, Rowitch DH (2012) Astrocytes and disease: a neurodevelopmental perspective. Genes Dev 26:891–907.

Morrow T, Song M-R, Ghosh A (2001) Sequential specification of neurons and glia by developmentally regulated extracellular factors. Development 128:3585–3594.

Nakashima K, Yanagisawa M, Arakawa H, Kimura N, Hisatsune T, Kawabata M, Miyazono K, Taga T (1999) Synergistic signaling in fetal brain by STAT3-Smad1 complex bridged by p300. Science 284:479–482.

Paşca AM, Sloan SA, Clarke LE, Tian Y, Makinson CD, Huber N, Kim CH, Park J-Y, O'Rourke NA, Nguyen KD, Smith SJ, Huguenard JR, Geschwind DH, Barres BA, Paşca SP (2015) Functional cortical neurons and astrocytes from human pluripotent stem cells in 3D culture. Nat Methods 12:671–678.

Polioudakis D et al. (2019) A Single-Cell Transcriptomic Atlas of Human Neocortical Development during Mid-gestation. Neuron 103:785-801.e8.

Reemst K, Noctor SC, Lucassen PJ, Hol EM (2016) The Indispensable Roles of Microglia and Astrocytes during Brain Development. Front Hum Neurosci 10:566.

Robinson MD, McCarthy DJ, Smyth GK (2010) edgeR: a Bioconductor package for differential expression analysis of digital gene expression data. Bioinformatics 26:139–140.

Rose CR, Felix L, Zeug A, Dietrich D, Reiner A, Henneberger C (2018) Astroglial Glutamate Signaling and Uptake in the Hippocampus. Frontiers in Molecular Neuroscience 10 Available at: https://www.frontiersin.org/article/10.3389/fnmol.2017.00451 [Accessed March 14, 2022].

Sawa A, Pletnikov MV, Kamiya A (2004) Neuron–glia interactions clarify genetic–environmental links in mental illness. Trends in Neurosciences 27:294–297.

Sloan SA, Andersen J, Paşca AM, Birey F, Paşca SP (2018) Generation and Assembly of Human Brain Region-Specific Three-Dimensional Cultures. Nat Protoc 13:2062–2085.

Sloan SA, Barres BA (2014) Mechanisms of astrocyte development and their contributions to neurodevelopmental disorders. Curr Opin Neurobiol 27:75–81.

Zhang Y, Sloan SA, Clarke LE, Caneda C, Plaza CA, Blumenthal PD, Vogel H, Steinberg GK, Edwards MSB, Li G, Duncan JA, Cheshier SH, Shuer LM, Chang EF, Grant GA, Gephart MGH, Barres BA (2016) Purification and Characterization of Progenitor and Mature Human Astrocytes Reveals Transcriptional and Functional Differences with Mouse. Neuron 89:37–53.